APMP 2012 Kyoto

Technical Digest of

the 7th Asia-PacificMicrowave Photonics

Conference (APMP2012)

April 25-27, 2012
Coop-Inn Kyoto, Kyoto, Japan

Sponsor:
Electronics Society, the Institute of Electronics, Information and Communication Engineers (IEICE)

Technical Co-sponsors:
IEEE Photonics Society Japan Chapter
IEEE Photonics Society Kansai Chapter
IEEE Microwave Theory and Techniques Society Japan Chapter
IEEE Microwave Theory and Techniques Society Kansai Chapter

Financial Co-sponsors:
Telecom Engineering Center (TELEC)
The Telecommunications Advancement Foundation (TAF)

Cooperation:
IEICE Technical Committee on Microwave and Millimeter-wave Photonics
IEICE Technical Group on Terahertz Application Systems

In this paper, we propose new electro-optic modulators operated with over 100 GHz wireless signals by using two-dimensional array of split-ring resonators. In the two-dimensional array of split-ring resonators on $LiNbO_3$ / $LiTaO_3$, which is one of the metamaterial structures, strong electric fields can be induced by irradiating a wireless millimetre-wave / terahertz-wave signals from above. By combining with guided-wave technology and polarization reversal technology, wireless-driven over 100 GHz optical modulators are obtainable. The analysis and expected performances are reported.

16:30-16:45

WD-3 Application of High-Power Photodiode-Arrays to 300 GHz-Band Wireless Link

Kazuki Arakawa*, Takuma Takada*, Kazumasa Miyake*, Ho-Jin Song**, Katsuhiro Ajito**, Naoya Kukutsu**, Tadao Nagatsuma*, **Osaka University, Japan, **NTT Microsystem Integration Laboratories, Japan*

This paper presents an application of high-power photodiode arrays to 300-GHz band wireless link which can be easily combined with ultra-broadband fiber-optic links. Requirement of output current and/or output power for the photodiode in this link is discussed. Using two-photodiode arrays, an error-free wireless transmission at a bit rate of 10 Gbit/s has experimentally been demonstrated with a photocurrent of as small as 2 mA for each photodiode, that is about a half of previous single photodiode.

16:45-17:00

WD-4 Design and Measurement of Plate Laminated Waveguide Slot Array Antennas in Millimeter and Sub-Millimeter Wave Regions

Dongjin Kim*, Jiro Hirokawa*, Makoto Ando*, Takuma Takada**, Tadao Nagatsuma**, Jun Takeuchi***, Akihiko Hirata***, **Tokyo Institute of Technology, Japan, **Osaka University, Japan, ***NTT Microsystem Integration Laboratories, Japan*

We design and fabricate double-layer slotted waveguide array antennas having wide bandwidths and high efficiencies for 120 GHz and 350 GHz frequency bands. To achieve high gain and high efficiency in extremely high frequency bands, the diffusion bonding technique of plate laminated waveguide is used as a fabrication method. The antennas having 16x16 slots show about 70% efficiency with 32 dBi gain and about 50% efficiency with 31 dBi gain in 120 GHz and 350 GHz frequency bands, respectively.

17:00-17:15

WD-5 Investigation of Optimal Silicon Avalanche Photodiode Pairs for 60-GHz Balanced Subharmonic Optoelectronic Mixers

Minsu Ko*, Myung-Jae Lee*, Holger Rucker**, Woo-Young Choi*, **Yonsei University, Republic of Korea, **IHP, Germany*

We characterize and compare common-N and common-P types of silicon avalanche photodiode pairs for 60-GHz balanced subharmonic optoelectronic mixer application. The common-N type has 4-dB higher up-conversion efficiency but the common-P type has 1.7 times wider 3-dB intermediate-frequency bandwidth.

17:15-17:30

WD-6 Speci c SMA Connected TO-Can FPLD Package for 6-GHz 256-QAM Direct Modulation

Yi-Cheng Li, Yu-Chieh Chi, Gong-Ru Lin, *National Taiwan University, Taiwan*

A specific SMA connector is used to connect the TO-can packaged FPLD for enhancing direct modulation bandwidth of 256-QAM up to 6-GHz with EAM and SNR of 1.5% and 32.5 dB respectively.

WD-5 APMP 2012, Kyoto
Apr. 25, 2012

Investigation of Optimal Silicon Avalanche Photodiode Pairs for 60-GHz Balanced Subharmonic Optoelectronic Mixers

Minsu Ko[*1], Myung-Jae Lee[*1], Holger Rücker[*2], and Woo-Young Choi[*1]

1. Yonsei University, Seoul 120-749, Korea. wchoi@yonsei.ac.kr
2. IHP, Im Technologiepark 25, 15236 Frankfurt (Oder), Germany.

***Abstract*—We characterize and compare common-N and common-P types of silicon avalanche photodiode pairs for 60-GHz balanced subharmonic optoelectronic mixer application. The common-N type has 4-dB higher up-conversion efficiency but the common-P type has 1.7 times wider 3-dB intermediate-frequency bandwidth.**

***Keywords*—Avalanche photodiode (APD), fiber-wireless system, silicon photonics, 60 GHz, subharmonic optoelectronic mixer (SHOEM).**

I. Introduction

Recently, 60-GHz wireless communications in silicon technologies have been actively investigated to meet demands for ever-increasing wireless data transmission capacity [1]. With this, fiber-wireless systems have attracted attention as they can extend the small coverage of 60-GHz wireless systems by distributing broadband data from a central office (CO) to remote antenna units (RAUs) via low-loss optical fiber [2]. Furthermore, adapting silicon photonics approaches for fiber-wireless systems is of great interest as this allows low-cost realization of integrated photonic and electronic devices. We have previously demonstrated 60-GH fiber wireless systems based on CMOS-compatible optoelectronic mixers [3].

A subharmonic optoelectronic mixer (SHOEM) using silicon photodetectors is an attractive component, which simultaneously photodetects optical intermediate-frequency (IF) signals and up-converts them into the 60-GHz band using 30-GHz local-oscillator (LO) signals [3]-[6]. We have previously demonstrated a balanced SHOEM by utilizing a silicon avalanche photodiode (APD) pair, which has much enhanced conversion efficiency than a single-APD SHOEM [6]. The schematics and the operation principle of the balanced SHOEM are shown in Figure 1. Since the APD pair acts as a frequency doubler for LO signals [7], IF photocurrents are up-converted into signals having $2f_{LO} \pm f_{IF}$ frequency components.

For the balanced SHOEM, two configurations for APD pairs are possible: common-N and common-P depending on the APD common RF output terminal as shown in Figure 2. In the common-N type, LO signals are injected into the anodes of the pair, and RF output signals are collected from the common cathode. In the common-P type, APDs are configured in the opposite direction as shown in Figure 2 (b) so that RF signals are collected from the common anode.

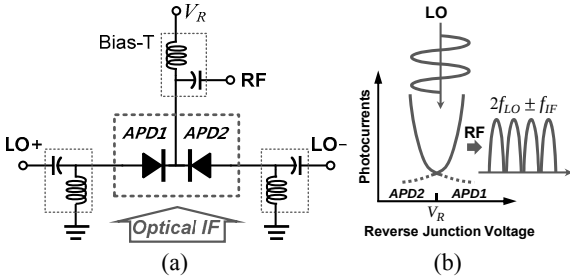

Figure 1. (a) Schematics and (b) operation principle of balanced SHOEM [6].

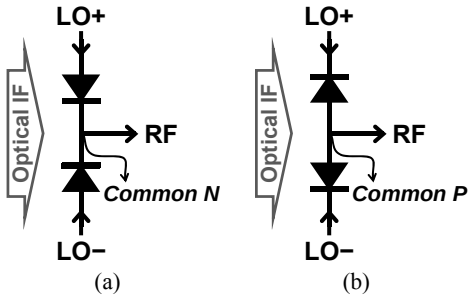

Figure 2. Device configurations of (a) common-N and (b) common-P silicon APD pairs.

In this paper, we compare the DC, AC, and 60-GHz up-conversion characteristics of above two types of balanced SHOEMs.

II. Device Structures

Two types of balanced SHOEMs were realized in IHP's 0.25-μm SiGe:C BiCMOS process [8]. Figure 3 shows the top-view layout and schematic cross-section of the common-N type. A pair of vertical PN junctions is formed by two separated P^+ regions and common N-well region. Each junction has the lateral dimension of 4 μm × 10 μm separated

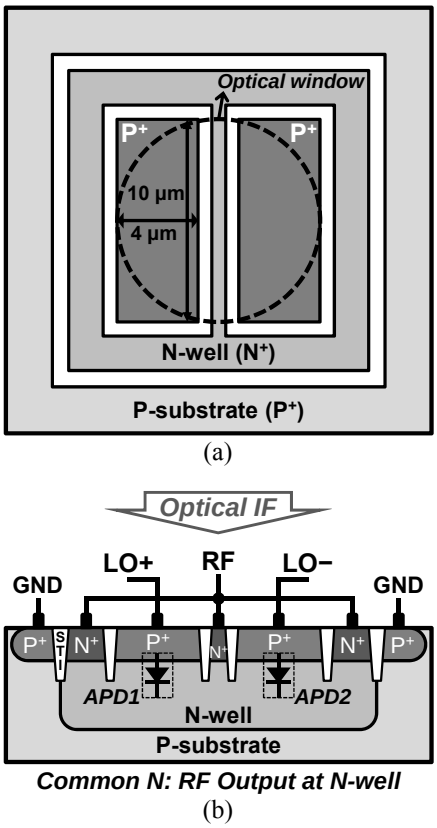

Figure 3. (a) Top-view layout and (b) schematic cross-section of common-N silicon APD pair.

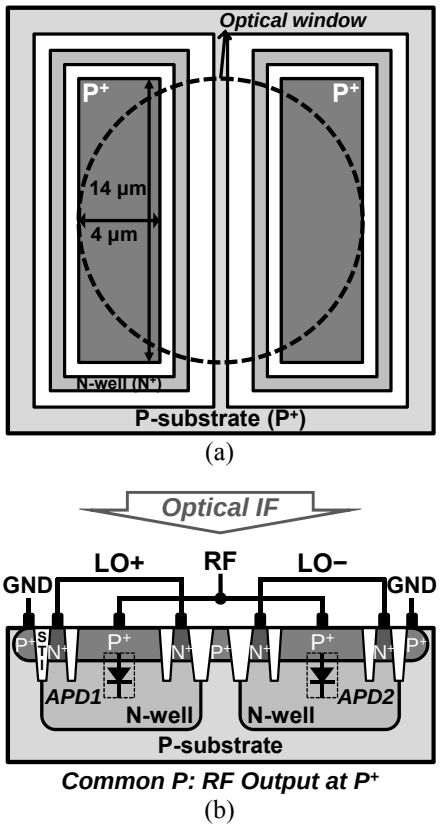

Figure 4. (a) Top-view layout and (b) schematic cross-section of common-P silicon APD pair.

by 2 μm. 850-nm optical signals are vertically injected into two APDs through a lensed fiber having a spot diameter of 10 μm. Photocurrents are extracted from common N-well and collected into the RF output terminal. Differential LO signals are applied to P^+ regions.

The top-view layout and schematic cross-section for the common-P type are shown in Figure 4. Two separated N-well regions form independent cathodes for differential LO input signals. They are separated by 6 μm so that they are not affected by dopant diffusion. Each junction has the lateral dimension of 4 μm × 14 μm. RF output is collected from P^+ region in each N-well.

III. Measured Results and Discussions

A. DC Characteristics

Figure 5 shows current-voltage characteristics of two types of silicon APD pairs under illumination and dark conditions. For illumination, 1 mW of 850-nm light was injected into devices. Avalanche breakdown voltages of two types have the same value of 11.2 V. The common-N type has much higher currents than the common-P type before avalanche breakdown. This is because both P^+/N-well junction and N-well/P-substrate junction contribute to output currents. N-well/P-substrate junction generates larger drift and diffusion currents than P^+/N-well junction because of lower doping concentration and larger charge neutral region [9]. The difference in currents decreases as avalanche currents in P^+/N-well junctions become larger near avalanche breakdown. Figure 6 shows responsivities near the breakdown. At the maximum point, the responsivities of 3.34 and 1.84 are obtained for common-N and common-P type, respectively. The common-N type has 5.2-dB higher maximum responsivity than the common-P type.

B. AC Characteristics

Devices were characterized by using a vector network analyzer and an electro-optical modulator to generate optical AC signals. The average optical power injected into the device was 1 mW. Figure 7 shows relative photodetection frequency responses of two types at maximum avalanche gain bias. The common-N type has 5.1-dB higher photodetection response at low frequencies, but the common-P type has 1.7 times wider 3-dB bandwidth. Discrepancies of two responses can be by two factors: frequency-independent decrease of 2.7 dB in the common-P type and frequency-dependent increase of 2.4 dB at low frequencies in the common-N type.

The frequency-independent decrease in the common-P type is caused by inefficient optical coupling. As shown in Figure 3 and Figure 4, the common-P type requires more spacing to separate two APDs than the common-N type. Therefore, the common-P type absorbs less light than the common-N type, resulting in frequency-independent

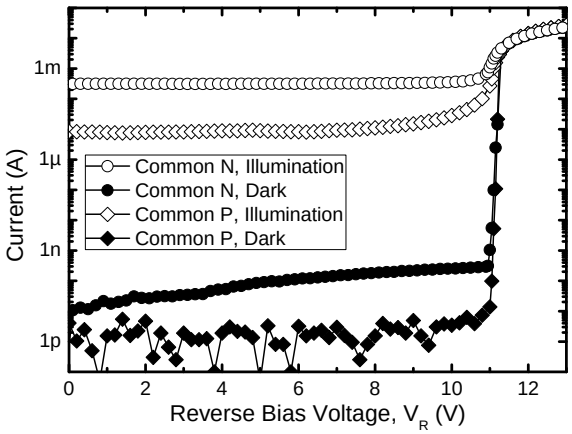

Figure 5. Current-voltage characteristics of common-N (circles) and common-P (diamonds) APD pairs under illumination (hollow) and dark (filled) conditions.

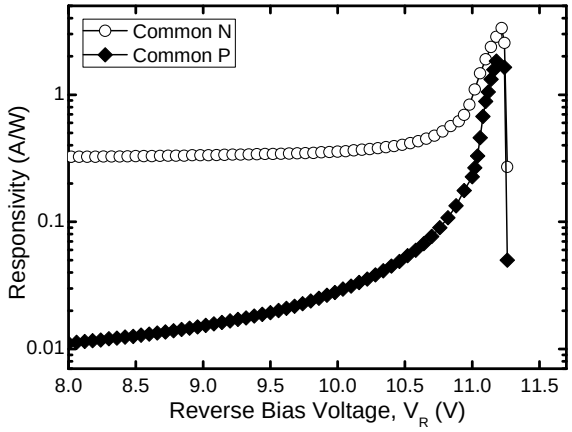

Figure 6. Responsivities of common-N (circles) and common-P (diamonds) APD pairs.

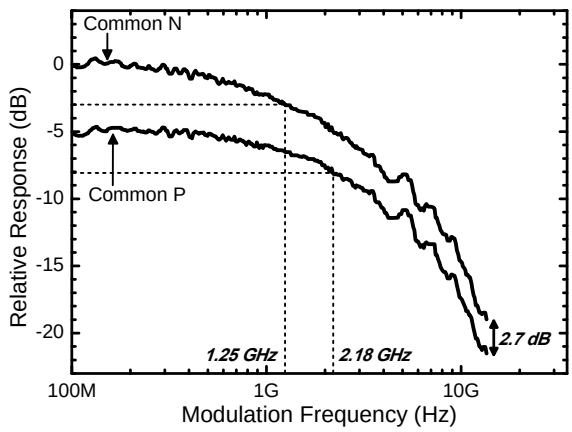

Figure 7. Relative photodetection frequency responses of common-N and common-P APD pairs at maximum avalanche gain bias. Inset is normalized responses.

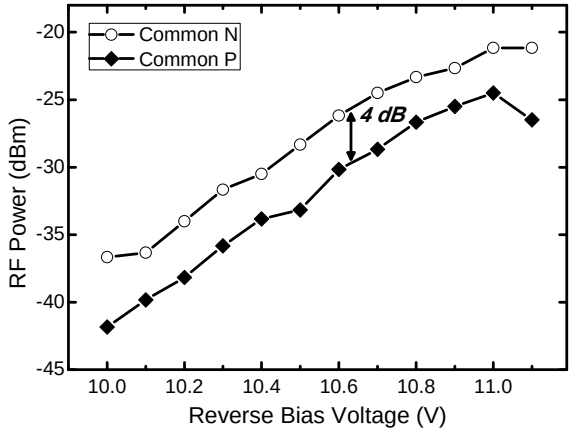

Figure 8. 60.1-GHz up-converted RF signal powers of common-N (circles) and common-P (diamonds) APD pairs at different reverse bias voltages.

loss in the photodetection response.

The frequency-dependent increase in the common-N type originates from N-well/P-substrate junction effect. As mentioned earlier, N-well/P-substrate junction increases total photocurrents of the common-N type, so it increases the photodetection response at low frequencies. However, because carriers generated in this junction reach the output terminal by slow diffusion process [9], the increase vanishes at high frequencies, resulting in a decrease in the 3-dB bandwidth from 2.18 GHz to 1.25 GHz.

C .Up-Conversion Characteristics

100-MHz optical IF signals and 18-dBm 30-GHz LO signals are used for up-conversion measurements. Figure 8 shows 60.1-GHz up-converted RF signal powers of two types at different reverse bias voltages. The up-converted power increases as the reverse bias voltage increases, and it maximizes at 11.0 V. The common-N type has 4-dB higher up-conversion efficiency than the common-P type, and the results have consistency with the measured DC and AC characteristics.

IV. CONCLUSION

We characterize common-N and common-P silicon APD pairs in terms of DC current-voltage relationship and responsivity, AC photodetection frequency response, and 60-GHz up-conversion efficiency. The common-N type shows better up-conversion performance and the common-P type shows wider 3-dB bandwidth performance. This observation will be very useful for selecting the optimal device structure of silicon APD pairs for given applications.

Acknowledgement

This work (2010-0014798) was supported by Mid-career Researcher Program through NRF grant funded by the MEST. The authors are very thankful to IDEC for EDA software support.

References

[1] A. M. Niknejad, "Siliconization of 60 GHz," *IEEE Microwave Mag.*, vol. 11, pp. 78-85, Febrary 2010.

[2] H. Ogawa, D. Polifko, and S. Banba,

"Millimeter-wave fiber optics systems for personal radio communication," *IEEE Trans. Microwave Theory & Tech.*, vol. 40, no. 12, pp. 2285-2293, December 1992.

[3] H.-S. Kang and W.-Y. Choi, "Fibre-supported 60 GHz self-heterodyne systems based on CMOS-compatible harmonic optoelectronic mixers," *Electronics Letters*, vol. 43, no. 20, pp. 1101-1103, September 2007.

[4] M. J. Lee, H. S. Kang, K. H. Lee, and W. Y. Choi, "Self-Oscillating Harmonic Opto-Electronic Mixer Based on a CMOS-Compatible Avalanche Photodetector for Fiber-Fed 60-GHz Self-Heterodyne Systems," *IEEE Trans. Microwave Theory & Tech.*, vol. 56, no. 12, pp.3180-3187, December 2008.

[5] J.-Y. Kim, M.-J. Lee, and W.-Y. Choi, "60GHz CMOS-APD Optoelectronic Mixers with Optimized Conversion Efficiency," *in Proc. 2010 IEEE Int. Topical Meeting Microwave Photonics*, pp. 139-142, October 2010.

[6] M. Ko, J.-Y. Kim, M.-J. Lee, H. Rücker, and W.-Y. Choi, "A Silicon Balanced Subharmonic Optoelectronic Mixer for 60-GHz Fiber-Wireless Downlink Application," *IEEE Photonics Technology Letters*, vol. 23, no. 23, pp. 1805-1807, December 2011.

[7] S. A. Maas, Nonlinear Microwave and RF Circuits, 2nd ed., Norwood, MA: Artech House, 2003.

[8] B. Heinemann, R. Barth, D. Knoll, H. Rücker, B. Tillack, and W. Winkler, "High-performance BiCMOS technologies without epitaxially-buried subcollectors and deep trenches," *Semiconductor Science & Technology*, vol. 22, no. 1, pp. S153-S157, January 2007.

[9] M.-J. Lee and W.-Y. Choi, "Performance Comparison of Two Types of Silicon Avalanche Photodetectors Based on N-well/P-substrate and P^+/N-well Junctions Fabricated With Standard CMOS Technology," *Journal of the Optical Society of Korea*, vol. 15, no. 1, pp. 1-3, March 2011.